SYSTEMATIC CORRECTION MECHANISM OF GEOMETRIC DISTORTIONS IN THE KITSAT-1 CCD EARTH IMAGES

Impyeong Lee†, Taejung Kim†, Soon D. Choi‡
Research Fellow†, Director‡
Satellite Technology Research Center (SaTReC)
Korea Advanced Institute of Science and Technology(KAIST)
373-1, Kusung-dong, Yusung-Ku, Taejon, 305-701, Korea
e-mail: iplee@satrec.kaist.ac.kr, tjkim@satrec.kaist.ac.kr

Commission III, Working Group III/1

KEYWORDS: **Remote_Sensing, Correction, Modeling, Distortion, Satellite, Geometric, Precision**

ABSTRACT

The CCD Earth Image Experiment (CEIE) is one of the main payload of the KITSAT-1, an experimental micro-satellite. Since it was launched on Oct. 10, 1992, the CEIE has taken more than 500 images on the Earth surface world-wide so far. An image from space is very different from a feature on the real Earth surface due to diverse radiometric and geometric distortions. Preprocessing to remove those distortions has to take place before the image data is processed and analyzed further for various applications. The images from the KITSAT-1 are dramatically distorted due to very poor pointing ability of the satellite. Moreover, the attitude determination and control system (ADCS) of the KITSAT-1 does not give sufficiently accurate attitude information because it cannot have attitude sensors enough to do it due to the strict limitation of weight and volume like many other micro-satellites. Since many systematic geometric correction mechanisms developed previously use fully accurate attitude information, they could not be appropriate for images from micro-satellites such as the KITSAT-1. A new mechanism described here estimates attitude and position information reversibly using ground control points selected from satellite images and maps. Then, It establishes a geometric model based on the estimated information. This paper describes the procedure to perform geometric correction of the KITSAT-1 CCD earth images and shows the result from this mechanism.

Nomenclature

$[\ A\ ]_n$	the nth element of a matrix A.
(α_m,β_m)	the coordinates of the mth map ground control points
ϕ, η	the longitude and latitude of satellite ground position in C4 system
$\theta_1,\theta_2,\theta_3$	satellite attitude parameters, rotation angles for three axis
(x_m,y_m)	the coordinates of the mth image ground control points
A	a point on the CCD sensor
B	a point on the center of the lens
C1	the coordinate system defined on the CCD sensor
C2	the coordinate system defined on the satellite
C3	the coordinate system defined on the orbit
C4	the coordinate system defined on the Earth
C	a point on the surface of the Earth
$\mathbf{L}_{C2}$	the **L** vector expressed in C2 system
$\mathbf{L}_{C4}$	the **L** vector expressed in C4 system
L	a vector from the point A to the point B
M	a vector from the point B to the point C
R	the radius of the Earth
$\mathbf{R}_{23}$	a rotation matrix between C2 system and C3 system
$\mathbf{R}_{34}$	a rotation matrix between C3 system and C4 system
f	the focal length of the lens
h	satellite altitude
$\mathbf{p}_{n+1}$	the next predicted parameters from the current ones.
$\mathbf{p}_n$	the current estimated parameters
p	a vector including six geometric model parameters (θ_1, θ_2, θ_3, ϕ, η, h)

1. Introduction

The KITSAT-1, an experimental microsatellite, was launched successfully on Oct. 10, 1992 by Ariane v52. Its total mass is about 48.6 Kg and its dimension is 35.2 × 35.6 × 67.0 cm^3. Four payloads are on board it to carry out scientific and engineering experiments. They are CCD Earth Image Experiment (CEIE), Digital Signal Processing Experiment (DSPE), Cosmic Ray Experiment (CRE), and Digital Store and Forward Communication Experiment (DSFCE). All the payloads have worked well without any failure and shown interesting results so far.(Kim et. al,1993)(Lee et. al.,1993)

The CEIE consists of two different camera systems and a transputer based image processing system. The CCD camera systems use two aerial CCD sensor and capture meteorological scale monochrome images in a 568×576 pixel format. One of them has a wide view angle(96°) and low resolution(4 km×4 km per pixel). The other has a narrow view angle(12°) and high resolution(400m×400m per pixel).(Yoo,1994)

Since the KITSAT-1 was launched, the CEIE has taken of more than 500 images world-wide so far. However, some of them include abnormalities due to hardware and also many images have much cloud cover. Consequently, about 150 images were used for developing this geometric correction mechanism.

The preprocessing of remotely sensed data includes any process that has to take place before remote sensing data can be processed and analyzed by the scientific users for their own application objects. Data from remote sensing missions are not always optimal in quality. Each remote sensing system has its own characteristic capability depending on such things as the instrument design, altitude of the platform, and performance of the recording equipment. Other less predictable, often extraneous, influences may adversely affect the quality of the retrieved data. Preprocessing functions are necessary to reduce or eliminate such inadequacies. It consists of mainly two correction; radiometric correction and geometric correction. (Battett and Curtis,1982) (Curran,1985)

This paper describes the systematic correction mechanism of heavy geometric distortions inherent in images from micro-satellites with poor pointing ability. It also shows the result in case that this mechanism is applied to the KITSAT-1 images.

2. Background

Most of the earth images from a satellite are heavily distorted geometrically. These distortions are mainly from the Earth, the satellite, the orbit and the image projection. The Earth contributes to the image deformation by its rotation, oblateness, and curvature. The contribution of the satellite comes from its variation in speed, attitude, and altitude. The projection of a spherical surface on a flat image also gives rise to the geometric distortions. These deformations, if not properly accounted for, will prevent meaningful result in further image processing such as mosaic, classification, comparison or fusion with other images and so on.(Mather,1987)

Various geometric distortions inherent in remotely sensed images have been usually corrected by two methods. The first one is to use the sufficiently accurate geometric model based on the geometry of the sensor, the satellite, the orbit and the Earth. The second one is to use a simple polynomial derived from the relation in a set of ground control points (GCP) that correspond to those in real maps.(Muller,1988)

Many microsatellites like the KITSAT-1 carry experimental Earth imaging payloads. However, since they usually provide very limited information about their positions and attitudes due to insufficient and rather inaccurate sensors, this makes it difficult to perform accurate geometric corrections of their images using the first method. The images from those satellites have been mostly geometrically corrected using the second method, which may cause additional distortions in the corrected images because the derived polynomial used in the correction is too coarse to represent accurately the whole process causing geometric distortion.

The Attitude Determination and Control System(ADCS) of the KITSAT-1 stabilizes its attitude using gravity-gradient boom and uses several attitude sensors with coarse and indeterminate accuracy for attitude determination. The ADCS can provide just pointing error that explains how much the satellite pointing is deviated from the line between the satellite and the center of the Earth but cannot give directional information of the deviation. Since this makes unable to establish an accurate model for the KITSAT-1 image geometric distortion process, the second method was applied to carry out geometric correction but get just the results with poor accuracy.

The geometric model in the KITSAT-1 can be represented by mainly six uncertain parameters: the pitch, yaw and roll angles of the satellite attitude and the latitude, longitude and altitude of the satellite position. In particular, the parameters of the attitude information are indeterminate as the ADCS provides just pointing errors on its attitude. The uncertain parameter values of the KITSAT-1 geometric model are estimated by using a least mean squares algorithm to utilize the relationships of GCP selected between satellite images and real maps. Fig. 1 shows a flow chart of the systematic correction mechanism described here.

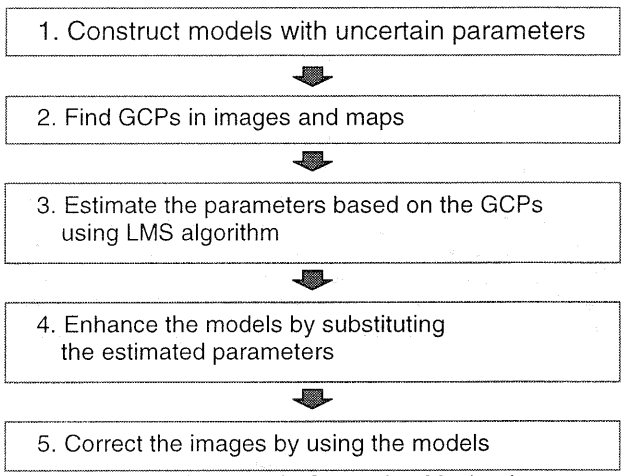

Figure 1. Systematic Correction Mechanism

3. Establishment of Geometric Model

Fig.2 shows the fundamental principle to establish the geometric model of the KITSAT-1 CCD cameras. Three points are defined on CCD sensor(**A**), on the center of the lens(**B**), and on the Earth surface(**C**). Let **L** and **M** be the vector from the point **A** to the point **B** and the vector from the point **B** to the point **C**, respectively. If the coordinates of the points **A** and **B** are known, it is possible to derive the coordinates of the point **C** from the condition that the vector **M** is parallel to **L** so that the point **C** may be imaged on the point **A** on the CCD sensor.

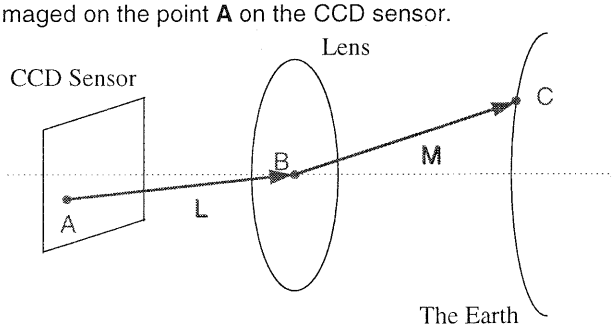

Figure 2. Fundamental Principle to Derive a Geometric Model

Four coordinate systems are defined on the CCD sensor, the satellite, the orbit and the earth respectively as shown in Fig. 3.

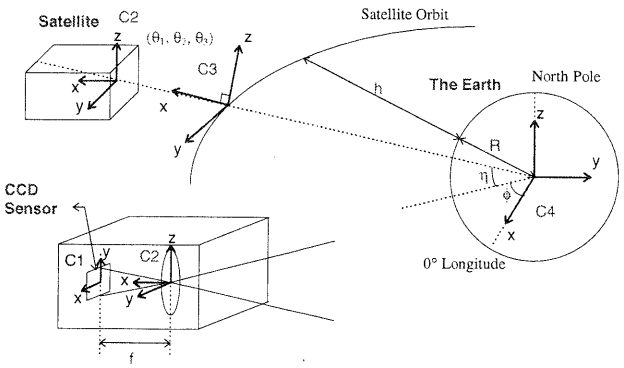

Figure 3. The Establishment of Four Coordinate Systems

Let the coordinates of a point on the CCD sensor denoted in C1 system be (x,y) and the longitude and latitude values of image appeared in the point be (α,β). If **T** is the function determined by the geometric model, it satisfies the relationships in that

$$T(x,y)=(\alpha,\beta) \quad (1)$$
$$T^{-1}(\alpha,\beta)=(x,y) \quad (2)$$

3.1 Non-inverse Geometric Model

The following procedures are to derive the function **T**. Since the coordinates of the point **A** is expressed in **C2** system as shown Eq.(3), the vector **L** can be denoted as Eq.(4).

$$\mathbf{A}=(x,y)_{C1}=(f,x,y)_{C2} \quad (3)$$
$$\mathbf{L}_{C2}=(0,0,0)-(f,x,y)=(-f,-x,-y)_{C2} \quad (4)$$

If the rotation matrix between the **C2** and **C3** system is denoted as $\mathbf{R}_{23}$ and the rotation matrix between the **C3** and **C4** system $\mathbf{R}_{34}$, the vector **L** is expressed in **C4** system as

$$\mathbf{L}_{C4}=\begin{bmatrix} l_x \\ l_y \\ l_z \end{bmatrix}=\mathbf{R}_{34}\mathbf{R}_{23}\mathbf{L}_{C2}$$
$$=\begin{bmatrix} c_4c_5 & -s_4 & -c_4s_5 \\ s_4c_5 & c_4 & -s_4s_5 \\ s_5 & 0 & c_5 \end{bmatrix}\begin{bmatrix} c_1c_2 & c_1s_2s_3+s_1c_3 & -c_1s_2c_3+s_1s_3 \\ -s_1c_2 & -s_1s_2s_3+c_1c_3 & s_1s_2c_3+c_1s_3 \\ s_2 & -c_2s_3 & c_2c_3 \end{bmatrix}\begin{bmatrix} -f \\ -x \\ -y \end{bmatrix} \quad (5)$$

where $c_1=\cos\theta_1$, $s_1=\sin\theta_1$, $c_2=\cos\theta_2$, $s_2=\sin\theta_2$, $c_3=\cos\theta_3$, $s_3=\sin\theta_3$, $c_4=\cos\phi$, $s_4=\sin\phi$, $c_5=\cos\eta$, and $s_5=\sin\eta$.

The position of the point **B** is nearly the same as the location of the satellite in **C4** system. The position of the satellite is found from

$$\mathbf{B}_{C4}=((R+h)c_5c_4,\ (R+h)c_5s_4,\ (R+h)s_5) \quad (6)$$

An arbitrary point C on the earth with certain longitude and latitude have the coordinates like

$$\mathbf{C}=(R\cos\beta\cos\alpha,\ R\cos\beta\sin\alpha,\ R\sin\beta) \quad (7)$$

The vector **M** that is from the point B to C is expressed as

$$\mathbf{M}=\mathbf{C}-\mathbf{B}=(R\cos\beta\cos\alpha-(R+h)c_5s_4,\ R\cos\beta\sin\alpha-(R+h)c_5s_4,\ R\sin\beta-(R+h)s_5) \quad (8)$$

The condition that the vector **M** is parallel to the vector **L** makes the following three relationships;

$$\begin{aligned} R\cos\beta\cos\alpha-(R+h)c_5c_4 &= kl_x \\ R\cos\beta\sin\alpha-(R+h)c_5s_4 &= kl_y \\ R\sin\beta-(R+h)s_5 &= kl_z \end{aligned} \quad (9)$$

where k is an arbitrary real number.

If $\cos\beta=0$, it implies the position on the north or the south pole and then the longitude value α is meaningless. If $\cos\beta\neq0$, the second order equation about k is derived from Eq.(9) and described as

$$k^2(l_x^2+l_y^2+l_z^2)+2k(-f(R+h)c_5c_4-l_x(R+h)c_5s_4-l_y(R+h)s_5)+(R+h)^2-R^2=0 \quad (10)$$

The value of $l_x^2+l_y^2+l_z^2$ never come to zero because the point A is the location coordinates of the satellite, the k can be evaluated by solving the second order equation of Eq.(10). At last, the α and β are derived from

$$\beta=\sin^{-1}\left(\frac{kl_z+(R+h)s_5}{R}\right)$$
$$\alpha=\tan2^{-1}\left(\frac{kl_y+(R+h)c_5s_4}{R\cos\beta},\ \frac{kl_x+(R+h)c_5c_4}{R\cos\beta}\right) \quad (11)$$

by substituting the k evaluated above. If the second order equation in Eq.(10) may produce two different solutions of k and then also of α and β, the proper one between two solution is one of the point with the shorter distance from the satellite. The function of **T** was then determined by the values derived in Eqs(3~11).

3.2 Inverse Geometric Model

The inverse function of the geometric model, $\mathbf{T}^{-1}$, is derived reversibly by using Eqs.(3~11). The vector $\mathbf{L}_{C4}$ is derived from Eq.(5) as

$$\mathbf{L}_{C4}=\begin{bmatrix} l_x \\ l_y \\ l_z \end{bmatrix}=\frac{\mathbf{W}}{k}$$
$$\text{where } \mathbf{W}=\begin{bmatrix} R\cos\beta\cos\alpha-(R+h)c_5c_4 \\ R\cos\beta\sin\alpha-(R+h)c_5s_4 \\ R\sin\beta-(R+h)s_5 \end{bmatrix} \quad (12)$$

Since $\mathbf{R}_{23}$ and $\mathbf{R}_{34}$ are rotation matrices between coordinate systems, they are orthogonal matrices.(Hughes) The vector $\mathbf{L}_{C2}$ is expressed from Eq.(5) as

$$\mathbf{L}_{C2}=\begin{bmatrix} -f \\ -x \\ -y \end{bmatrix}=\mathbf{R}_{23}^{-1}\mathbf{R}_{34}^{-1}\mathbf{L}_{C4}=\frac{1}{k}\mathbf{R}_{23}^{T}\mathbf{R}_{34}^{T}\mathbf{W} \quad (13)$$

The k, x and y can derived from Eq.(13) and described as

$$k=-\frac{1}{f}\left[\mathbf{R}_{23}^{T}\mathbf{R}_{34}^{T}\mathbf{W}\right]_1$$
$$\begin{bmatrix} x \\ y \end{bmatrix}=-\frac{1}{k}\left[\mathbf{R}_{23}^{T}\mathbf{R}_{34}^{T}\mathbf{W}\right]_{2,3} \quad (14)$$

The inverse function of the geometric model is then determined in Eqs.(12~14).

4. Estimation of Geometric Model Parameters

The geometric model described in the previous section has six unknown or uncertain parameters($\theta_1,\theta_2,\theta_3,\phi,\eta,h$). Those parameters can be estimated by using least mean square method based on the relationships of several ground control points between satellite images and maps. The inverse model is defined more simply than the non-inverse model since the inverse model interpretation solves a problem to find the intersections between a line and a plane but the non-inverse model interpretation does a problem to find those between a line and a spherical surface. Therefore, the inverse model was used for parameter estimation instead of the non-inverse model.

Several ground control points are selected by comparing satellite images with maps and denoted as (x_m, y_m) and (α_m, β_m) in satellite images and maps, respectively. Using these ground control points, the parameters ($\theta_1,\theta_2,\theta_3,\phi,\eta,h$) for the geometric model are to be estimated. The estimation is performed using a least mean squares algorithm repeatedly. The inverse geometric model with uncertain estimated parameters, ($\theta_1',\theta_2',\theta_3',\phi',\eta',h'$) produces ($x_m'$, y_m') with the input, (α_m, β_m) instead of the true value (x_m, y_m) from GCPs.

$$(x_m', y_m') = \mathbf{T}^{-1}(\theta_1',\theta_2',\theta_3',\phi',\eta',h';\alpha_m,\beta_m) \tag{15}$$

The error E of the estimation with uncertain parameters is defined as

$$E = \frac{1}{n}\sum_{m=1}^{n}(x_m'-x_m)^2 + (y_m'-y_m)^2 \tag{16}$$

where n is the total number of GCPs used for parameter estimation.

A least mean squares algorithm is used in order to determine the six parameters to minimize the error defined in Eq.(17). When performing parameter prediction repeatedly, the next parameters, $\mathbf{P}_{n+1}$, can be estimated from the current ones, $\mathbf{P}_n$, by using the relationship that

$$\mathbf{p}_{n+1} = \mathbf{p}_n - c\nabla E = \mathbf{p}_n - c\left(\frac{dE}{d\theta_1},\frac{dE}{d\theta_2},\frac{dE}{d\theta_3},\frac{dE}{d\phi},\frac{dE}{d\eta},\frac{dE}{dh}\right) \tag{17}$$

where c is a small converge factor.

The differential values substituted in Eq.(17) are to be derived in the following equations, Eqs.(18~21). If p_k is an arbitrary component $\mathbf{p}$, the differential value of the error E about p_k is described as

$$\frac{dE}{dp_k} = \frac{1}{n}\sum_{k=1}^{n}\left\{2(x_m'-x_m)\frac{dx_m'}{dp_k} + 2(y_m'-y_m)\frac{dy_m'}{dp_k}\right\} \tag{18}$$

Following equations are the differential values of x_n' and y_n' about each model parameter.

$$\begin{bmatrix}\frac{dx_n'}{d\theta_1}\\ \frac{dy_n'}{d\theta_1}\end{bmatrix} = \left[\frac{1}{k^2}\mathbf{R}_{23}^{\mathrm{T}}\mathbf{R}_{34}^{\mathrm{T}}\mathbf{W}\frac{dk}{d\theta_1}\right]_{2,3} - \left[\frac{1}{k}\frac{d\mathbf{R}_{23}^{\mathrm{T}}}{d\theta_1}\mathbf{R}_{34}^{\mathrm{T}}\mathbf{W}\right]_{2,3} \tag{19a}$$

$$\begin{bmatrix}\frac{dx_n'}{d\theta_2}\\ \frac{dy_n'}{d\theta_2}\end{bmatrix} = \left[\frac{1}{k^2}\mathbf{R}_{23}^{\mathrm{T}}\mathbf{R}_{34}^{\mathrm{T}}\mathbf{W}\frac{dk}{d\theta_2}\right]_{2,3} - \left[\frac{1}{k}\frac{d\mathbf{R}_{23}^{\mathrm{T}}}{d\theta_2}\mathbf{R}_{34}^{\mathrm{T}}\mathbf{W}\right]_{2,3} \tag{19b}$$

$$\begin{bmatrix}\frac{dx_n'}{d\theta_3}\\ \frac{dy_n'}{d\theta_3}\end{bmatrix} = \left[\frac{1}{k^2}\mathbf{R}_{23}^{\mathrm{T}}\mathbf{R}_{34}^{\mathrm{T}}\mathbf{W}\frac{dk}{d\theta_3}\right]_{2,3} - \left[\frac{1}{k}\frac{d\mathbf{R}_{23}^{\mathrm{T}}}{d\theta_3}\mathbf{R}_{34}^{\mathrm{T}}\mathbf{W}\right]_{2,3} \tag{19c}$$

$$\begin{bmatrix}\frac{dx_n'}{d\phi}\\ \frac{dy_n'}{d\phi}\end{bmatrix} = \left[\frac{1}{k^2}\mathbf{R}_{23}^{\mathrm{T}}\mathbf{R}_{34}^{\mathrm{T}}\mathbf{W}\frac{dk}{d\phi}\right]_{2,3} - \left[\frac{1}{k}\mathbf{R}_{23}^{\mathrm{T}}\left\{\frac{d\mathbf{R}_{34}^{\mathrm{T}}}{d\phi}\mathbf{W} + \mathbf{R}_{34}^{\mathrm{T}}\frac{d\mathbf{W}}{d\phi}\right\}\right]_{2,3} \tag{19d}$$

$$\begin{bmatrix}\frac{dx_n'}{d\eta}\\ \frac{dy_n'}{d\eta}\end{bmatrix} = \left[\frac{1}{k^2}\mathbf{R}_{23}^{\mathrm{T}}\mathbf{R}_{34}^{\mathrm{T}}\mathbf{W}\frac{dk}{d\eta}\right]_{2,3} - \left[\frac{1}{k}\mathbf{R}_{23}^{\mathrm{T}}\left\{\frac{d\mathbf{R}_{34}^{\mathrm{T}}}{d\eta}\mathbf{W} + \mathbf{R}_{34}^{\mathrm{T}}\frac{d\mathbf{W}}{d\eta}\right\}\right]_{2,3} \tag{19e}$$

$$\begin{bmatrix}\frac{dx_n'}{dh}\\ \frac{dy_n'}{dh}\end{bmatrix} = \left[\frac{1}{k^2}\mathbf{R}_{23}^{\mathrm{T}}\mathbf{R}_{34}^{\mathrm{T}}\mathbf{W}\frac{dk}{dh}\right]_{2,3} - \left[\frac{1}{k}\mathbf{R}_{23}^{\mathrm{T}}\mathbf{R}_{34}^{\mathrm{T}}\frac{d\mathbf{W}}{dh}\right]_{2,3} \tag{19f}$$

The differential values of k about each parameter included in Eq.(19) is described in the following equations.

$$\left[\frac{dk}{d\theta_1}\right] = -\left[\frac{1}{f}\frac{d\mathbf{R}_{23}^{\mathrm{T}}}{d\theta_1}\mathbf{R}_{34}^{\mathrm{T}}\mathbf{W}\right]_1 \tag{20a}$$

$$\left[\frac{dk}{d\theta_2}\right] = -\left[\frac{1}{f}\frac{d\mathbf{R}_{23}^{\mathrm{T}}}{d\theta_2}\mathbf{R}_{34}^{\mathrm{T}}\mathbf{W}\right]_1 \tag{20b}$$

$$\left[\frac{dk}{d\theta_3}\right] = -\left[\frac{1}{f}\frac{d\mathbf{R}_{23}^{\mathrm{T}}}{d\theta_3}\mathbf{R}_{34}^{\mathrm{T}}\mathbf{W}\right]_1 \tag{20c}$$

$$\left[\frac{dk}{d\phi}\right] = -\left[\frac{1}{f}\mathbf{R}_{23}^{\mathrm{T}}\left\{\frac{d\mathbf{R}_{34}^{\mathrm{T}}}{d\phi}\mathbf{W} + \mathbf{R}_{34}^{\mathrm{T}}\frac{d\mathbf{W}}{d\phi}\right\}\right]_1 \tag{20d}$$

$$\left[\frac{dk}{d\eta}\right] = -\left[\frac{1}{f}\mathbf{R}_{23}^{\mathrm{T}}\left\{\frac{d\mathbf{R}_{34}^{\mathrm{T}}}{d\eta}\mathbf{W} + \mathbf{R}_{34}^{\mathrm{T}}\frac{d\mathbf{W}}{d\eta}\right\}\right]_1 \tag{20e}$$

$$\left[\frac{dk}{dh}\right] = -\left[\frac{1}{f}\mathbf{R}_{23}^{\mathrm{T}}\mathbf{R}_{34}^{\mathrm{T}}\frac{d\mathbf{W}}{dh}\right]_1 \tag{20f}$$

The differential values of the matrix or vector included Eq.(19~20) are denoted as follows.

$$\left[\frac{d\mathbf{R}_{23}^{\mathrm{T}}}{d\theta_1}\right] = \begin{bmatrix}-S_1C_2 & -S_1S_2S_3+C_1C_3 & S_1S_2C_3+C_1S_3\\ -C_1C_2 & -C_1S_2S_3-S_1C_3 & C_1S_2C_3-S_1S_3\\ 0 & 0 & 0\end{bmatrix}^{\mathrm{T}} \tag{21a}$$

$$\left[\frac{d\mathbf{R}_{23}^{\mathrm{T}}}{d\theta_2}\right] = \begin{bmatrix}-C_1S_2 & C_1C_2C_3 & -C_1C_2C_3\\ S_1S_2 & -S_1C_2S_3 & S_1C_2C_3\\ C_2 & S_2S_3 & -S_2C_3\end{bmatrix}^{\mathrm{T}} \tag{21b}$$

$$\left[\frac{d\mathbf{R}_{23}^{\mathrm{T}}}{d\theta_3}\right] = \begin{bmatrix}0 & C_1S_2C_3-S_1S_3 & C_1S_2S_3+S_1C_3\\ 0 & -S_1S_2C_3-C_1S_3 & -S_1S_2S_3+C_1C_3\\ 0 & -C_2C_3 & -C_2S_3\end{bmatrix}^{\mathrm{T}} \tag{21c}$$

$$\left[\frac{d\mathbf{R}_{34}^{\mathrm{T}}}{d\phi}\right] = \begin{bmatrix}-S_4C_5 & -C_4 & S_4S_5\\ C_4C_5 & -S_4 & -C_4S_5\\ 0 & 0 & 0\end{bmatrix}^{\mathrm{T}} \tag{21d}$$

$$\left[\frac{d\mathbf{R}_{34}{}^{T}}{d\eta}\right]=\begin{bmatrix}-s_4c_5 & 0 & -c_4c_5\\ -s_4s_5 & 0 & -s_4c_5\\ c_5 & 0 & -s_5\end{bmatrix}^{T} \quad (21e)$$

$$\left[\frac{d\mathbf{W}}{d\phi}\right]=(R+h)\begin{bmatrix}c_5s_4\\ -c_5c_4\\ 0\end{bmatrix} \quad (21f)$$

$$\left[\frac{d\mathbf{W}}{d\eta}\right]=(R+h)\begin{bmatrix}s_5c_4\\ s_5s_4\\ -c_5\end{bmatrix} \quad (21g)$$

$$\left[\frac{d\mathbf{W}}{dh}\right]=\begin{bmatrix}c_5c_4\\ c_5s_4\\ -s_5\end{bmatrix} \quad (21h)$$

The model parameters are assumed to satisfy the following conditions about the satellite attitude and position.

Cond. (i) the satellite pointing is not deviated in amount of more than 12 degrees from the line between the satellite and the center of the Earth.

Cond. (ii) the position of the satellite predicted from the orbital model allow only less than 2° error for the longitude and latitude and less than 30km error for the altitude of the actual position.

If the deviated angle is δ, the ***Cond. (i)*** is described mathematically as

$$\delta=\tan^{-1}\left(\frac{\sqrt{\mathbf{R}_{23,21}{}^{2}+\mathbf{R}_{23,31}{}^{2}}}{\mathbf{R}_{23,11}}\right)=\tan^{-1}\left(\frac{\sqrt{(c_1c_2)^2+(-s_1c_2)^2}}{s_2}\right)\le 12^\circ \quad (22)$$

The ***Cond. (ii)*** is described mathematically as

$$\begin{aligned}|\phi-\phi_0|&\le 2^\circ\\ |\eta-\eta_0|&\le 2^\circ\\ |h-h_0|&\le 30\text{km}\end{aligned} \quad (23)$$

where ϕ_0,η_0, and h_0 are expected parameters from the orbital model of the KITSAT-1.

The model parameters are estimated repeatedly by using Eq.(17) with the conditions in the Eq.(22~23). The systematic correction based on the estimated parameter values was applied to remove the geometric distortions in the KITSAT-1 images.

5. Result

Following several pictures shows some geometrically corrected results of a wide angle camera image over the southern Europe, taken by the KITSAT-1 on May 8, 1995. Fig. 4 shows just a raw image. Fig. 5 shows the geometrically corrected image drawn in latitude and longitude grids. The model parameters to correct this image were estimated as

θ_1: -10.6551°, θ_2: 0.0361°, θ_3: 32.1341°

ϕ: 28.3961°E, η: 40.9716°N, h: 1290.06Km

The pointing error of the satellite at the time when this image was captured is calculated by using Eq.(22) and it is about 10.6552°. The corrected image is projected on the Mercator map in Fig. 6. The white lines on the figure are coast lines in a real map.

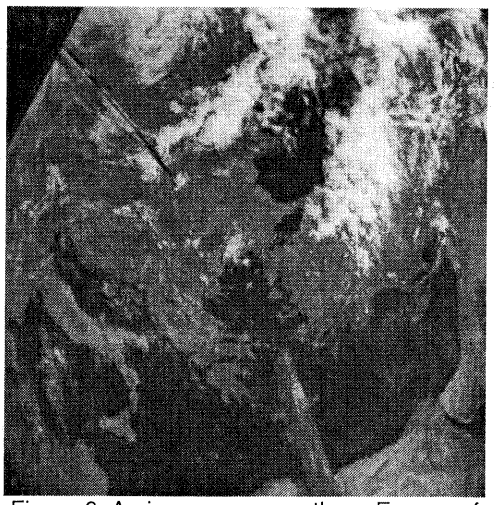

Figure 6. An image over southern Europe of the KITSAT-1

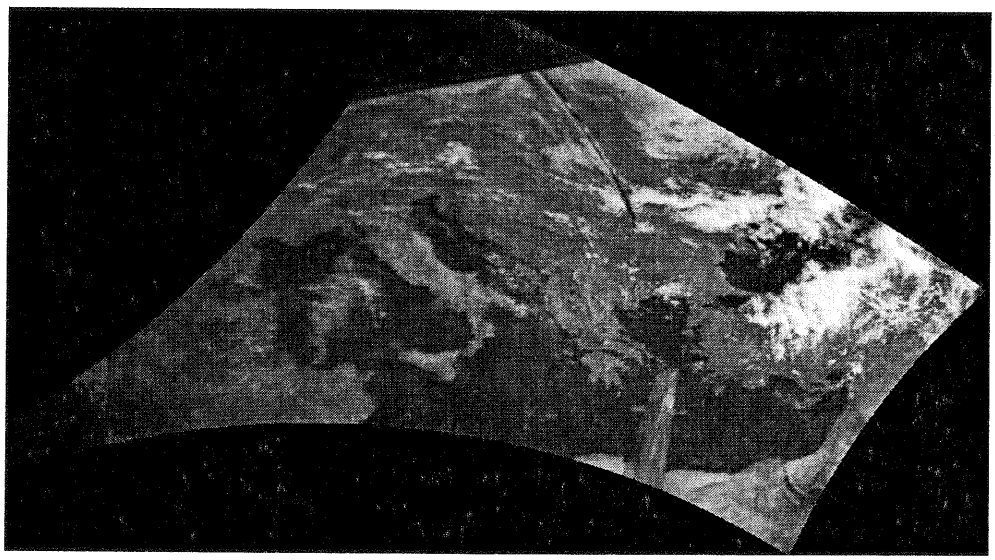

Figure 7. The preprocessed corrected image

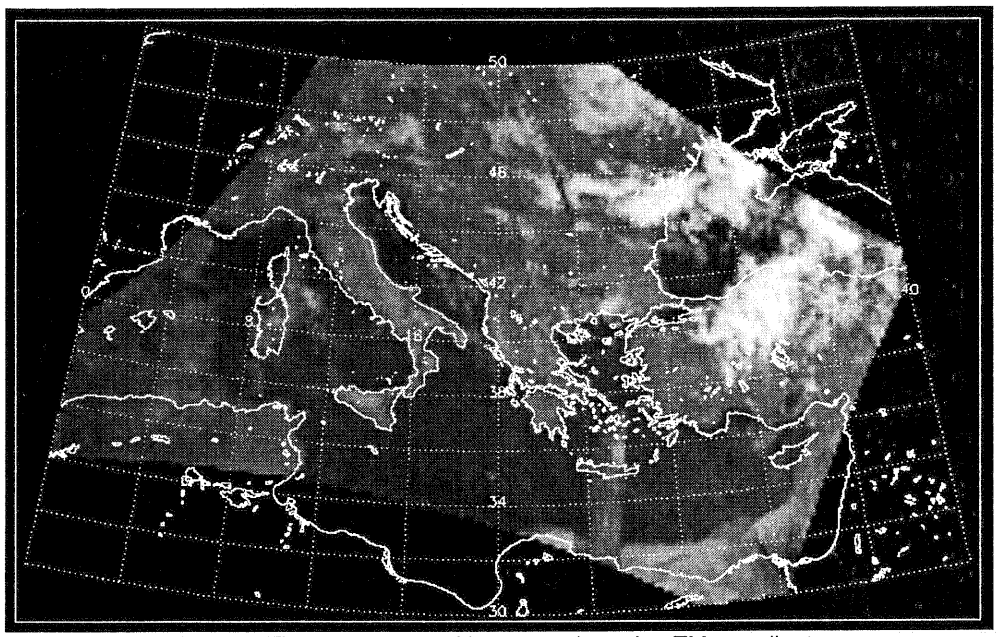

Figure 8. The preprocessed image projected to TM coordinates

This correction mechanism described here is applied to many images from the KITSAT-1. In most cases, the mechanism finds successfully the geometric model parameters with less than 0.01 pixel accuracy after about more than 10000 iterations to converge them. This result shows much better performance comparing with simple linear polynomial GCP mapping.

6. Conclusions

The CEIE in the KITSAT-1 microsatellite demonstrates many possibilities in the observation of the Earth surface with a very low cost satellite platform and imager. Images from the CEIE can be very valuable even if they are not comparable to scenes from existing commercial satellites. They show some hardware abnormalities but produce lots of images with reasonable qualities and low cloud coverage, which can be used for further processing and analysis

Preprocessing is very necessary to use an image for various applications. In this paper, the geometric distortions in the KITSAT-1 images were analyzed and a correction mechanism to remove them is developed. The developed procedure shows reasonable performance in correcting image from micro-satellites such as the KITSAT-1 images. It can be also a basis for developing geometric correction algorithms for images from other remote sensing satellites which have large amount of pointing error or do not give sufficient accurate attitude information.

Reference

Barrett E.C. and Curtis L.F., 1982, Introduction to Environmental Remote Sensing 2nd Ed., Chapman and Hall Ltd.

Curran, P.J., 1985, Principles of Remote Sensing, John Wiley & Sons Inc.

Hughes P.C., Spacecraft Attitude Dynamics, John Wiley & Sons

Kim, S.H., Sung, D.K. and Choi, S.D., 1992, A Korean Experimental Microsatellite - KITSAT-1 System, AP-MCST

Lee, I., Sung, D. K. and Choi, S.D., 1993, Multimission Experimental Microsatellites - KITSAT Series, the 7th Annual AIAA/USU Conference on Small Satellites

Mather, P.M., 1987, Computer Processing of Remote Sensed Images (An Introduction), John Wiley & Sons

Muller, J.P., 1988, Digital Image Processing in Remote Sensing, Taylor & Francis Inc.

SPOT Image, 1988, SPOT User's Handbook - Volume 1 Reference Manual, CNES and SPOT Image

Ward, J., 1991, The UO-22 Earth Imaging System, The AMSAT Journal, Vol.14, No.6, pp. 1~7

Yoo S.K., 1992, Earth Imaging System - Camera Head, SaTReC Internal Document, Vol. 6A-CAM